The Antiphasic Regulatory Module Comprising *CDF5* and its Antisense RNA *FLORE* Links the Circadian Clock to Photoperiodic Flowering

Rossana Henriques[1,2,*], Huan Wang[1], Jun Liu[1,3], Marc Boix[2], Li-Fang Huang[1] and Nam-Hai Chua[1,*]

[1] Laboratory of Plant Molecular Biology, The Rockefeller University, 1230 York Avenue, New York, NY 10065-6399, USA; [2] Centre for Research in Agricultural Genomics, Consortium CSIC-IRTA-UAB-UB, Carrer de la Vall Moronta, Edifici CRAG, 08193 Bellaterra (Cerdanyola del Vallés), Barcelona, Spain; [3] National Key Facility for Crop Resources and Genetic Improvement, Institute of Crop Science, Chinese Academy of Agricultural Sciences, Beijing 100081, China

***Authors for correspondence:**
Rossana Henriques; Email: rossana.henriques@cragenomica.es; Tel.: +34 935636600
and
Nam-Hai Chua; Email: chua@mail.rockefeller.edu; Tel.: +1 2123278126

Heading: Circadian long non-coding RNAs promote rhythmicity robustness within natural antisense transcript pairs

Total word count	6688	No. of figures	6 (all in colour)
Summary	199	No. of Tables	0
Introduction	884	No of Supporting Information files	2 (Fig S1-S7; Table S1-S3; Notes S1-S3)
Material and Methods	1192		
Results	2992		
Discussion	1529		
Acknowledgements	91		

This is the accepted version of the following article: Henriques, R. et al. "The antiphasic regulatory module comprising CDF5 and its antisense RNA FLORE links the circadian clock to photoperiodic flowering" in New phytologist, vol. 216, issue 3 (Nov. 2017), p. 854-867, which has been published in final form at DOI 10.1111/nph.14703. This article may be used for non-commercial purposes in accordance with Wiley Terms and Conditions for Self-Archiving.

Summary

- Circadian rhythms of gene expression are generated by the combinatorial action of transcriptional and translational feedback loops as well as chromatin remodelling events. Recently, long non-coding RNAs (lncRNAs) that are natural antisense transcripts (NATs) to transcripts encoding central oscillator components were proposed as modulators of core clock function in mammals (*Per*) and fungi (*frq*/*qrf*). Although oscillating lncRNAs exist in plants, their functional characterization is at an initial stage.

- By screening an *Arabidopsis thaliana* lncRNA custom-made array we identified *FLORE* (*CDF5 LONG NON-CODING RNA*), a circadian-regulated lncRNA that is a NAT of *CDF5*. Quantitative real-time RT-PCR confirmed the circadian regulation of *FLORE*, whereas *GUS*-staining and flowering time evaluation were used to determine its biological function.

- *FLORE* and *CDF5* antiphasic expression reflects mutual inhibition similarly to *frq*/*qrf*. Moreover, whereas the CDF5 protein delays flowering by directly repressing *FT* transcription, *FLORE* promotes it by repressing several *CDF*s (*CDF1*, *CDF3*, *CDF5*) and increasing *FT* transcript levels, indicating both *cis* and *trans* function.

- We propose that the *CDF5/FLORE* NAT pair constitutes an additional circadian regulatory module with conserved (mutual inhibition) and unique (function *in trans*) features, able to fine-tune its own circadian oscillation, and consequently, adjust the onset of flowering to favourable environmental conditions.

Key words

Circadian clock, long non-coding RNA, natural antisense transcripts, flowering time, *CDF*s

Introduction

Initially described as the "dark matter" of the genome, long non-protein coding RNAs (lncRNA) have emerged as novel regulators of development, disease and differentiation processes in animals. LncRNAs can originate from intergenic or intronic regions, or from the opposite strand of coding genes to which they have sequence complementarity being natural antisense transcripts (NATs) (Lee, 2012; Sabin *et al.*, 2013; Fatica & Bozzoni, 2014). Functional studies revealed a mechanism of lncRNA action based either on chromatin remodelling events (Heo & Sung, 2011; Csorba *et al.*, 2014), reshaping of nuclear organization (Rinn & Guttman, 2014), RNA processing (Bardou *et al.*, 2014), RNA stability (Ha & Kim, 2014), translational regulation (Jabnoune *et al.*, 2013), protein complex assembly, or protein subcellular location, all of which rely on their ability to bind nucleic acids and proteins.

In plants, lncRNA identification surpasses their functional characterization, although mounting evidence on tissue-, environmental- and developmental-specific expression patterns suggests important biological functions (Franco-Zorrilla *et al.*, 2007; Ariel *et al.*, 2014; Wang, H *et al.*, 2014; Ariel *et al.*, 2015; Bazin & Bailey-Serres, 2015; Shafiq *et al.*, 2016). *IPS1* (*INDUCED BY PHOSPHATE STARVATION 1*) is the first *Arabidopsis* lncRNA shown to sequester miR399 thereby regulating phosphate homeostasis (Franco-Zorrilla *et al.*, 2007). *Arabidopsis* lncRNAs are also involved in the vernalization-dependent flowering response due to the transcriptional modulation of *FLC* (*FLOWERING LOCUS C*) (Song, J *et al.*, 2012). *COOLAIR* (*COLD INDUCED LONG ANTISENSE INTRAGENIC RNA*) and *COLDAIR* (*COLD-ASSISTED INTRONIC NON-CODING RNA*) promote the repressive function of the PHD/PRC2 complex [PHD (homeodomain) proteins/POLYCOMB REPRESSIVE COMPLEX 2] in the *FLC locus* in response to cold (Swiezewski *et al.*, 2009; Heo & Sung, 2011; Song, J *et al.*, 2012). *COLDWRAP* (*cold of winter-induced noncoding RNA from the promoter*) was recently shown to associate with *COLDAIR* to form a repressive chromatin loop at the *FLC locus* (Kim & Sung, 2017). However, the identification of other lncRNAs revealed a wider functional landscape. *HID1* (*HIDDEN TREASURE 1*) moderately regulates the expression of the *PIF3* (*PHYTOCHROME-INTERACTING FACTOR 3*) transcription factor (Wang, Y *et al.*, 2014); and *APOLO* (*AUXIN REGULATED PROMOTER LOOP*) regulates *PID* (*PINOID*) expression by modulating chromosome loop dynamics thereby affecting auxin signalling (Ariel *et al.*, 2014). In addition, *ASCO*-RNA (*ALTERNATIVE*

SPLICING COMPETITOR RNA) regulates alternative splicing during lateral root formation in *Arabidopsis* (Bardou *et al.*, 2014).

Genome-wide studies using custom-made NATs arrays showed that approximately 70% of *Arabidopsis* protein-coding loci encode predicted NAT pairs (Wang, H *et al.*, 2014). NAT pair components can be protein-coding transcripts, a protein-coding transcript and lncRNA, or two lncRNAs. NATs can affect gene expression by different mechanisms; 1) regulation of transcription; 2) altering mRNA processing; 3) double strand RNA formation and silencing; and 4) RNA:RNA interaction in the cytoplasm (Magistri *et al.*, 2012; Zhang *et al.*, 2013). However, studies linking NAT pairs with chromatin marks also suggest a role in epigenome modification via small RNA-independent pathways (Luo *et al.*, 2013).

Because of their diverse functions, lncRNAs can participate either in long-term or more dynamic biological processes. This is the case of light-responsive lnc-NATs in *Arabidopsis*, as well as circadian-regulated lncRNAs expressed in the rat pineal gland (Coon *et al.*, 2012; Wang, H *et al.*, 2014). In addition, in the fungus *Neurospora*, the mutual inhibition between the clock master regulator *frequency* (*frq*) and its NAT lncRNA *qrf* forms a double negative feedback loop (Kramer *et al.*, 2003) that interconnects with the core clock and is pivotal for the maintenance and robustness of rhythmicity (Xue *et al.*, 2014). A proper running clock is paramount for optimal growth and development, since this internal timekeeper mechanism anticipates most of the daily and seasonal environmental changes (Dodd *et al.*, 2005; Doherty & Kay, 2010). In *Arabidopsis*, the circadian clock relies on several interconnected transcriptional loops where chromatin remodelling events contribute to the generation of robust circadian rhythms (Hemmes *et al.*, 2012; Malapeira *et al.*, 2012; Song & Noh, 2012; Foo *et al.*, 2016). Similarly to rat and *Neurospora*, oscillating transcripts from *Arabidopsis* non-coding genomic regions including NATs for central oscillator components have also been reported, however their function still remains unknown (Hazen *et al.*, 2009).

Here, we identified the antiphasic NAT pair comprising *FLORE* (*CDF5 LONG NON-CODING RNA*) and the *CDF5* (*CYCLING DOF FACTOR 5)* transcript. As members of the DOF (DNA-BINDING WITH ONE FINGER) family of plant specific transcription factors (Yanagisawa, 2002; Le Hir & Bellini, 2013), CDFs link the circadian clock to the photoperiodic flowering pathway due to their direct binding and inhibition of *CO* (*CONSTANS*) and *FT* (*FLOWERING LOCUS T*) promoters (Fornara *et al.*, 2009; Song *et al.*, 2015). The antiphasic expression of the *CDF5/FLORE* NAT pair reflects a mutual inhibitory regulation, which directly impacts flowering time regulation. *FLORE* is specifically expressed in the vasculature, where it not only regulates *CDF5* (its natural target in *cis*) but also *CDF1* and *CDF3* in *trans*. In addition to their circadian regulation, *FLORE* and *CDF5* mutual inhibition also seems to be important for the maintenance of their rhythmic expression patterns. We propose that the mutual regulation within antiphasic NAT pairs could be a conserved mechanism devised to help maintain robust circadian rhythms of each antisense transcript. In plants it would constitute an extra regulatory layer which limits the accumulation of important regulators to a precise time of the day and thus fine-tune fundamental processes such as the time to flower.

Material and Methods

Plant growth conditions and flowering time determination

Plants were grown in light (145 μmolm^{-2}s^{-1}), temperature (22ºC) and humidity (65%) controlled chambers under the following photoperiods; LD (Long day, 16h light/ 8h dark), SD (Short day, 8h light/16h dark) and 12L/D (12h light/12h dark). All plant growth conditions were as previously described (Kiba *et al.*, 2007; Kiba & Henriques, 2016). Seeds were surfaced sterilized and plated on a modified MS medium supplemented with 1% of sucrose. After plating, seeds were stratified for 4 days in the dark at 4ºC. All the flowering time experiments were performed at least two times with 10-15 seedlings per genotype, in different growth chambers to rule out any positional effects. In this case seeds were directly germinated in soil and stratified for the same period of time as in *in vitro* conditions. The *Arabidopsis thaliana* Columbia (Col-0) ecotype was used as wild-type (WT) for all the experiments. The *ddc*, *polIV*, *polV*, *dcl3-1*, *dcl2dcl4*, *rdr2-1* and *drb4-2* mutants are all in the Col-0 background and were previously described (Cao *et al.*, 2003; Xie *et al.*, 2004; Kanno *et al.*, 2005; Onodera *et al.*, 2005; Xie *et al.*, 2005; Jakubiec *et al.*, 2012). The *cdf-quadruple* mutant as well as *pSUC2::CDF5* (Fornara *et al.*, 2009) overexpressing lines were a kind gift from Dr. Coupland of the MPI, Germany.

The isolated *flore-prom* mutant (Sail_275_A10) carried a T-DNA inserted at 142bp from the transcriptional start site of *FLORE*. Homozygous plants were isolated by PCR screening and depletion in *FLORE* expression confirmed by qPCR. A similar strategy was followed for the *cdf5-prom* mutant (Salk_099079) where the T-DNA was inserted at 795bp into the *CDF5* promoter and the *cdf5-5'utr* (Salk_044252) mutant where the T-DNA insertion occurred at 239bp from the *CDF5* translational start site. Primers used for mutant isolation are described in Table S1.

Identification of cycling noncoding genes in *Arabidopsis*

The ATH lincRNA v1 array contained 15,744 60-mer oligonucleotide probes (Liu *et al.*, 2012). We used the previously reported protocol to profile lncRNA expression in *Arabidopsis* (Liu *et al.*, 2012; Wang, H *et al.*, 2014). A detailed description of the hybridization protocol is given in Supporting Information Methods S1. Hybridization images were scanned using the Agilent Feature Extraction Software to extract raw signal intensities of microarray probes. We applied the GeneSpring software with the Quantile method to normalize signal intensities of the ATH lincRNA v1 arrays. Using R-3.2.0 with the JTK_cycling package (Hughes *et al.*, 2010) we measured cycling pattern significance of the normalized signal intensities with Benjamini-Hochberg adjustment. Genes with the adjusted P-values lower than 0.05 (Adjusted P-value < 0.05) were considered as cycling genes. The high-throughput datasets used in this study were uploaded to Gene Expression Omnibus database under accession numbers GPL13750 and GSE80094. A summary of the results from this study is given in Notes S1.

Cloning of *FLORE* and *CDF5* and generation of transgenic lines

FLORE lncRNA expressed sequence was cloned using the cDNA synthesis kit SuperScript™ III First-Strand Synthesis System for RT-PCR (Invitrogen) with specific primers designed for the At1g69572 "other RNA" sequence, in order to account for strand specificity. The *FLORE* promoter was cloned using the 2kb fragment just upstream of the *FLORE* 5' transcriptional start site. Genomic cloning of *FLORE* was generated by DNA amplification of promoter and expressed sequence together. All these constructs were produced using the pENTR™ Directional TOPO® Cloning kit (Invitrogen) so as to generate the ENTRY Gateway® clones, which were transferred to their destination vectors following the manufacturer's instructions. For vascular tissue expression we used *pSUC2-GW* (Fornara et al., 2009), whereas *pH7WG2* (Karimi *et al.*, 2002) was used for 35S promoter driven constitutive expression, *pKGW* (Karimi *et al.*,

2002) was used for genomic cloning and *pBGWFS7* and *pKGWFS7* (Karimi *et al.*, 2002) for *promoter:GUS* fusions.

We used a different strategy to exchange promoters. Briefly, we used a two-step cloning strategy: first the *FLORE* promoter was amplified adding *Eco*RV and *Aat*II sites at its 5' and 3' end respectively. Then this fragment was ligated to the amplified *CDF5* genomic fragment with a C-terminal FLAG tag with *Aat*II and *Avr*II sites added at its 5' and 3'end respectively. The resulting *Eco*RV-*FLOREp*(*Aat*II):(*Aat*II)*CDF5*-*Avr*II fragment was cloned into the promoter-less pBa002a vector previously digested with *Eco*RV and *Avr*II. After confirmation by sequencing, all constructs were introduced into the *Agrobacterium* strain ABI50. Plant transformation and selection of primary transformants were performed as previously described (Zhang *et al.*, 2006). All the primers used for cloning are described in Table S2.

GUS staining assay

pFLORE:GUS transgenic plants were grown under selective medium for segregation analysis. Transgenic lines displaying a 3:1 ratio, indicative of a single insertion were amplified and used for *GUS* staining as described previously (Osnato *et al.*, 2012).

Quantification of RNA expression by qPCR

Expression analyses were done using reverse transcription followed by quantitative real time RT (Reverse Transcription)-PCR (qPCR) using either strand specific cDNA (*FLORE* detection) or oligodT cDNA (*CDF5* and all other protein-coding genes). Both types of cDNA were generated with the AffinityScript QPCR cDNA synthesis kit (Agilent). Each cDNA was then diluted 1:20 and 1µl used for each reaction, in a 10 µl final volume using the SYBR *Premix Ex Taq* Tli RNase H Plus (Takara). qPCR cycling was as follows, 94 ºC for 30 s followed by 40 cycles of 94ºC for 10 s, 60 ºC for 30 s, and a final step for melting curve determination (94 ºC for 15 s, ramping up from 60 ºC to 94 ºC with 0.5 ºC increments for 15 s). qPCR reactions were performed in a C1000 Thermal Cycler CFX96 Real Time System (BioRad) or a LightCycler® 480II (Roche) with identical results.

Gene expression was calculated using the $2^{-\Delta\Delta Ct}$ method where the results were first normalized with *Actin2* (At3g18780) and the lowest WT (Col-0) expression value was used as reference (value of 1) to which all the other samples were compared, unless otherwise stated. *IPP2* (Imaizumi *et al.*, 2005) has also been used to normalize samples with identical results to *Actin2*, which was then used as the preferential control. In this study the primer pairs designed to evaluate *FLORE* transcript amplified the splicing variant described in TAIR10 (At1g69572) unless otherwise stated. In order to accurately show the circadian expression pattern of each transcript we present the results from one representative experiment. However, in Notes S2 we show the biological replicates for some of the qPCR data presented in Fig. 1 and Fig. 5.

A detailed description of the qPCR protocol using fragment specific standard curves is given in Methods S2. Primers used in all qPCR reactions are listed in Table S3.

Small RNA Northern

The small RNA Northerns were performed as described previously (Jakubiec *et al.*, 2012). Briefly, small RNAs were extracted from plant tissue using Trizol and separated on a 15% polyacrylamide, 8M urea, 1x TBE gel. *CDF5/FLORE* PCR fragments were labelled using the Rediprime kit (Amersham) and purified with the mini Quick spin columns (Roche). Pre-hybridization and hybridization were performed at 42ºC overnight with the ULTRAhyb-Oligo Hybridization Buffer (Ambion). Normally three wash steps of 30 min at 42ºC each were done using a 1xSSC/0.1%SDS solution. Signal was detected on a PhosphorImager (Storm, GE Healthcare).

Results

FLORE and *CDF5* constitute a circadian-regulated Natural Antisense Transcript (NAT) pair

We identified thousands of lncRNAs in *Arabidopsis* by analysis of RNA-seq and tiling array datasets. For their further characterization we designed a custom oligonucleotide array to detect 4959 highly confident lncRNAs (Liu *et al.*, 2012). The array also contained probes for 309 TAIR annotated lncRNAs, 173 pre-miRNAs and protein-coding genes, such as the central oscillator components *LHY*, *CCA1* and *TOC1*. To identify oscillating lncRNAs we used this array to profile lncRNA expression under short day conditions (SD; 8h light/16h dark). Signal intensities of probes for positive control transcripts, including those of *CCA1* and *TOC1*, exhibited the expected rhythmic patterns, confirming the detection quality of our experiments (Notes S1). Applying the JTK_cycling programme (Hughes *et al.*, 2010) we found 928 noncoding transcripts with significant cycling expression patterns (Adjusted *P*-value < 0.05), and within this group were 744 lncRNAs (Notes S1). Signal intensities of the 3 probes targeting *FLORE* showed a 24h-period cycling pattern, confirming reproducibility in biological and technical replicates. These results indicate that a large number of lncRNAs in *Arabidopsis*, including *FLORE*, are cycling transcripts.

The *FLORE* transcript (1,163 nt) encodes a partial peptide of 35 amino acids with no identifiable domains (Kong *et al.*, 2007), no similarities with other *Arabidopsis* proteins (BLASTX; http://blast.ncbi.nlm.nih.gov) and that was not identified in genome-wide analyses of ribosome-associated open reading frames (Hsu *et al.*, 2016). These results suggested that *FLORE* is a novel lncRNA with a genomic location antisense to *CDF5* (Fig. 1a). We further determined that *FLORE* and *CDF5* are antiphasic circadian-regulated transcripts by reverse transcription followed by quantitative real-time RT-PCR (qPCR) in wild-type (WT; Col-0) plants grown under different photoperiods (SD, Long Day, LD, 16h light/8h dark) and circadian free-running conditions (continuous light, LL) (Fig. 1b-e). *CDF5* peaked at early morning (ZT0-ZT3) both under 12h light/ 12h dark (12 L/D) or long day (LD) conditions, whereas *FLORE* transcripts increased after ZT3 until their peak at ZT15 under 12L/D or ZT9-ZT12 under LD (ZT, *Zeitgeber* Time). We found that *FLORE* transcript levels were maintained during the beginning of the dark period and decreased towards dawn both under SD and 12L/D conditions. However, under LD *FLORE* transcript levels diminished around dusk and remained mostly unaltered during the dark period (Fig. 1d). In addition, under SD conditions *CDF5* expression showed a phase advance peaking at ZT21, whereas *FLORE* accumulated at higher levels from ZT9 to ZT15 (Fig. 1b). Sequence homology searches revealed that *FLORE* corresponds to the *locus* identifier At1g69572 described as encoding *other RNA* (TAIR10, https://www.arabidopsis.org/index.jsp). We cloned *FLORE* and identified a mixed population of cDNAs corresponding to four splicing variants with different intron size or intron retention (Fig. S1a). Under SD conditions, all *FLORE* splicing variants displayed an antiphasic expression pattern in relation to *CDF5* expression (Fig. S1b, c). We also analysed *FLORE* and *CDF5* transcript levels in *CCA1*-overexpressing plants that are affected in their circadian clock. Confirming their circadian regulation, we failed to detect the typical *FLORE* and *CDF5* oscillation pattern in these plants grown under LL conditions (Fig. 1f).

CDF5 negatively regulates _FLORE_ transcript levels

Despite their circadian regulation, the antiphasic expression of *FLORE* and *CDF5* also suggested mutual inhibition. To dissect this relationship we manipulated the transcript levels of *FLORE* and *CDF5*, either by T-DNA insertional mutagenesis or overexpression, followed by evaluation of the other partner circadian expression pattern. Since the available *cdf5-1* mutant (Fornara *et al.*, 2009) carries a T-DNA insertion in the overlapping region of *CDF5* and *FLORE*, we isolated two novel T-DNA insertion mutants in non-overlapping regions of *CDF5*. In *cdf5-prom* (Salk_099079) the T-DNA is inserted 795 bp upstream of its transcriptional start site whereas in *cdf5-5'utr* (Salk_044252) it disrupts the *CDF5* 5' untranslated region (*5'utr*) being inserted 239bp upstream of its translation start site (Fig. 2a). We then determined *CDF5* and *FLORE* expression in both mutants and WT plants during a 24h cycle (Fig. 2b-c). In *cdf5-prom* plants *CDF5* levels were lower (2-4 fold) than WT levels during most of the light period (ZT0 to ZT12) and we detected a slight phase advance, with *CDF5* peaking at ZT3 in these mutants. However, from ZT15 to ZT21 the *CDF5* transcript amount in these plants was similar to that of WT; conversely, *FLORE* still maintained its antiphasic expression pattern with transcript levels close to WT levels, with the exception of ZT0 and ZT21 where they were reduced approximately 2-fold (Fig. 2b). In *cdf5-5'utr* mutants we found extremely low levels of *CDF5* transcript when compared with WT plants. In these mutant plants, *FLORE* transcripts increased 2-4 fold from ZT9 to ZT18, although the oscillation pattern was still maintained (Fig. 2c). These results show that only a strong reduction in *CDF5* transcript amount is accompanied by an increase in the amplitude of *FLORE* expression. Furthermore, promoter insertion events differently affected *CDF5* transcription most likely due to the partial loss of regulatory motifs in this region. Consequently, *FLORE* expression was only slightly affected in these plants.

We then determined the effect of *CDF5* overexpression by analysing *pSUC2::CDF5* (*CDF5*-Ox) seedlings that accumulated *CDF5* specifically in phloem companion cells (Fornara *et al.*, 2009). In these plants *FLORE* transcripts showed a 3-fold reduction at peak time (ZT9-ZT12) but maintained their characteristic waveform although with reduced amplitude (Fig. 2d). Oppositely, in *cdf1-RNAi cdf2-1 cdf3-1 cdf5-1* quadruple mutants (*cdf-q*) (Fornara *et al.*, 2009), *FLORE* transcript levels were higher from ZT0 to ZT6 (1.6-7 fold) and, although they did not exceed WT levels at the peak (ZT9-ZT12), they were maintained close to peak levels from ZT9 to ZT18, that is 6h longer than the peak value present in WT plants (Fig. 2d). Taken together these results indicate that *CDF5*, and most likely other *CDF*s (*CDF1*, *CDF2* and *CDF3*), negatively regulate *FLORE* transcript levels.

FLORE accumulation in the vascular tissue regulates _CDF_s

We then examined the effects of modulating *FLORE* levels on *CDF5* transcript accumulation. We initially expressed *FLORE* from the *SUC2* (*SUCROSE TRANSPORTER 2*) promoter (Imlau *et al.*, 1999) and isolated two independent homozygous lines (*pSUC2::FLORE #2.8* and *pSUC2::FLORE #4.2*) (Fig. 3a; Fig. S2a). We found a 10-12 fold increase in *FLORE* levels (*pSUC2::FLORE #2.8*) which correlated with a 2-4 fold reduction in *CDF5* expression from ZT0-ZT9 (Fig. 3a). In *pSUC2::FLORE #4.2* seedlings, a 2-4 fold increase in *FLORE* transcripts repressed *CDF5* transcript levels by 1.4-1.6 fold, with a phase delay leading to *CDF5* peaking at ZT6 (Fig. S2a). We then searched for T-DNA insertion mutants in the *FLORE locus* but due to the complete overlap and sequence homology within the NAT pair (Fig. 1a), we were restricted to the *FLORE* promoter region, since other tools such as RNAi could also not be used. We could isolate the *flore-promoter* (*flore-prom*) mutant (SAIL_275_A10), where the T-DNA was inserted 142bp upstream of the *FLORE* transcriptional start site (and 71bp downstream from the *CDF5 3'UTR*). Similar to the *cdf5-prom* mutants, T-DNA insertion into the *FLORE* promoter differentially affected *FLORE* transcript levels throughout the 24h period (Fig. S3a). In fact, *flore-prom* mutants grown under LD conditions showed an increase (1.4-2.6 fold) in *FLORE* expression during the day and a reduction (2.5-5.7 fold) during the dark period (Fig. S3a). Moreover, we found in these plants a reduction in transcript levels of *CDF5* (1.6-6 fold), *CDF1* (1.3-1.6 fold) and *CDF3* (1.4-1.8 fold) mostly during the light period (Fig. S3b). Possibly, in *flore-prom* mutants the T-DNA insertion event lead to partial loss of *FLORE* transcriptional regulation that was then reflected in *CDF* (*CDF1*, *CDF3* and *CDF5*) altered expression. These results suggest that *FLORE* could act in *cis* to modulate *CDF5* transcript levels, but also in *trans* by affecting *CDF1* and *CDF3* expression.

Considering that *CDF*s are a vascular tissue-specific transcripts (Fornara *et al.*, 2009), we investigated the *FLORE* promoter activity using a *GUS* reporter system. We found that the *FLORE* promoter (2Kb upstream of its transcriptional start site)-*GUS* fusion was also expressed in the vascular tissue of leaves, stems, roots, sepals and petals (Fig. 3b-d). These results show that both transcripts of this NAT pair accumulated in the vasculature, which strengthens our hypothesis of mutual regulation. This regulation could also expand to other *CDF*s (*CDF1*, *CDF3*), as we have previously shown in *flore-prom* mutants (Fig. S3b). In agreement with this, in *FLORE* overexpressing plants both *CDF1* and *CDF3* transcripts oscillated with reduced amplitude displaying a 2-fold inhibition at their peak times (Fig. 3e). Therefore, our results indicate that *FLORE* accumulation in the vascular tissue modulates *CDF* expression, in *cis* (*CDF5*) and *trans* (*CDF1*, *CDF3*).

***CDF5/FLORE* reciprocal inhibition is required for maintenance of their circadian oscillation**

Tissue-specific modifications of either *FLORE* or *CDF5* transcript levels affected their partner expression waveform, mostly by reducing its amplitude but without a total loss of oscillation, indicating that a circadian-dependent regulatory mechanism was still present. However, this mutual repression within the NAT pair could also contribute to maintain robust circadian waving patterns. To evaluate this, we created an imbalance in the *CDF5/FLORE* relationship using components of the NAT pair. We expressed *CDF5* under the control of the *FLORE* promoter, introduced this construct into the *cdf5-5'utr* mutant (Fig. 4a) and evaluated the resulting circadian waveforms. We confirmed that *cdf5-5'utr* mutants showed low endogenous *CDF5* expression (Fig. 4b). On the other hand, in the *cdf5-5'utr/pFLORE::CDF5-FLAG #2.1* line the *CDF5* transcripts arising from the *FLORE* promoter displayed an altered circadian oscillation accumulating at high levels throughout the 24h period. Nevertheless, their circadian waveform did not perfectly mimic the *FLORE* expression pattern, suggesting the existence of other mechanisms of transcriptional and/or post-transcriptional regulation. Consequently, in these plants *FLORE* transcript levels were reduced 2-4 fold from ZT6 to ZT18, when compared to the *cdf5-5'utr* mutant (Fig. 4c). These results show that *CDF5* mis-expression throughout the day dampens the *FLORE* circadian waveform, further suggesting that the reciprocal inhibition within this NAT pair contributes to the proper oscillation of both transcripts.

The antiphasic *CDF5*/*FLORE* module constitutes an additional link in circadian-dependent regulation of flowering time

As CDF proteins can directly inhibit *CO* and *FT* transcription and delay flowering (Imaizumi *et al.*, 2005; Sawa *et al.*, 2007; Song, YH *et al.*, 2012), we did a comprehensive analysis of the flowering time phenotype of all our *CDF5* and *FLORE* mutants and transgenic lines grown under different photoperiods. We found that depletion of *CDF5* in *cdf5-5'utr* mutants resulted in a slightly early flowering phenotype, similar to the available single mutations or RNAi lines of either *cdf1*, *cdf2*, *cdf3* and *cdf5* (Imaizumi *et al.*, 2005; Fornara *et al.*, 2009) (Fig. 5a). These results further strengthen the notion of functional redundancy within the *CDF* family. Therefore, we then determined how modulating *FLORE* transcript amounts impacted on flowering time regulation. In *flore-prom* mutants grown under LD conditions we detected a weak early flowering phenotype determined by rosette leaf number (Fig. 5b). Most likely this is due to the slight reduction in *CDF1*, *CDF3* and *CDF5* transcript levels during the light period, when CDF protein transcriptional activity is more relevant (Fig. S3b).

We then examined the flowering time phenotype of *pSUC2::FLORE* overexpressing plants grown under LD and SD conditions. Both *pSUC2::FLORE* lines (#2.8 and #4.2) showed early flowering under the two photoperiods tested (Fig. 5c, d; Fig. S2b, d). In these plants we found a small increase in *CO* transcript levels (1.4-3 fold) and a higher accumulation of *FT* levels (2-3 fold) under LD (Fig. 5e; Fig. S2c). This stronger effect on *FT* expression could depend both on the accumulation of higher *CO* transcript levels and the inhibition of *CDF* (*CDF1*, *CDF3* and *CDF5*) expression in *pSUC2::FLORE* lines. The relevance of *CDF* inhibition is shown in *cdf-q* mutants where we observed a stronger accumulation of *FT* transcripts (3.9-25.8 fold) and a somewhat weaker effect on *CO* transcript levels (1.9-12.6 fold) (Notes S3). Similarly, under SD conditions, the *pSUC2::FLORE* lines displaying early flowering phenotype also accumulated higher (2.35-14.3 fold) *FT* transcript levels (Fig. S2d, e).

We further confirmed this phenotype by generating a transgenic line in which *FLORE* was expressed from its own native promoter (*pFLORE::FLORE #3.3*). Similar to *pSUC2::FLORE*, these plants also displayed an early flowering phenotype under LD, although this phenotype was not as strong compared to *FLORE* overexpressing plants

(Fig. S2f). Then, we investigated how misexpression of *CDF5* in *cdf5-5'utr/pFLORE::CDF5-FLAG #2.1* plants would affect flowering time. We found that, under LD, the early flowering phenotype of *cdf5-5'utr* mutants was reverted to late flowering when *CDF5* expression was transcribed from the *FLORE* promoter (Fig. 5f). This delay in flowering was mirrored by an inhibition in *FT* transcript levels that decreased below WT and *cdf5'-5'utr* mutant values (Fig. 5g). *FT* transcript levels have to rise above a threshold at an inductive ZT time (ZT12-ZT20) for a period of several days, in order to promote the expression of floral identity genes in the apical meristem and induce flowering (Krzymuski *et al.*, 2015). Therefore, this reduction in *FT* expression could account for the late flowering phenotype of *cdf5-5'utr/pFLORE::CDF5-FLAG #2.1* plants. Together, these results show that the reciprocal inhibition between *FLORE* and *CDF5* also reflects an opposite biological function that could add a new regulatory layer of flowering time control.

CDF5/FLORE most likely act by a siRNA-independent mechanism

The sequence complementarity between *FLORE* and *CDF5* in *cis*, as well as its sequence homology with other *CDF* targets in *trans*, suggested a mechanism based on the generation of small interfering RNAs (nat-siRNAs) by processing of a putative *CDF5/FLORE* double-strand RNA. However, this mechanism is not consistent with the antiphasic oscillation of *FLORE* and *CDF5* since nat-siRNA accumulation could continuously target either or both transcripts thereby preventing their accumulation every 24h. To see if RNA-dependent silencing mechanisms could contribute to the antiphasic expression of *FLORE* and *CDF5* we used four different approaches; 1) evaluation of available data of small RNAs derived from this *locus*, either in siRNA biogenesis pathway mutants or associated with specific ARGONAUTE proteins; 2) expression of *FLORE* under the control of a strong 35S promoter to evaluate siRNA generation and flowering time; 3) determination of *FLORE* and *CDF5* transcript circadian waveforms in different mutants affected either in siRNA biogenesis [*dicer-like3-1 (dcl3-1)*, *dcl2dcl4* (Xie *et al.*, 2004; Xie *et al.*, 2005)], *trans*-acting siRNA (ta-siRNA) generation [*double-stranded RNA binding protein4-2* (*drb4-2*) (Jakubiec *et al.*, 2012)], and the RdDM (RNA-dependent DNA Methylation) pathway [*drm1drm2cmt3* (*ddc)*, *rna polymerase IV* (*polIV)*, *polV* (Cao *et al.*, 2003; Kanno *et al.*, 2005; Onodera *et al.*, 2005)] grown under

12 L/D conditions; and 4) determination of the absolute levels of *FLORE* and *CDF5* transcripts in these mutants at both peak and trough time points.

Firstly, we queried the available small RNAs (smRNAs) databases (Mi *et al.*, 2008; Montgomery *et al.*, 2008) but did not uncover any smRNA that would perfectly map to both genomic and mRNA sequences of *CDF5* and *FLORE*.
Secondly, we expressed *FLORE* under the control of the CaMV35S promoter (*p35S::FLORE #2.2* and *p35S::FLORE #3.6*) in order to promote its high accumulation and abolish its circadian waving pattern (Fig. S4a). We investigated siRNA accumulation in both lines by small RNA Northern, using labelled fragments derived from the NAT pair overlapping region. We tested two time points (ZT3 and ZT18), when *FLORE* and *CDF5* transcript levels were diminishing but still present, and a transcriptional regulatory mechanism could be at play. In WT plants, siRNAs were not detected in either time points, although in *p35S::FLORE* transgenic lines siRNAs accumulated at higher levels in line #2.2 and weakly in line #3.6 (Fig. S4b). Flowering time evaluation under LD conditions did not reveal any statistically significant changes, suggesting that, similarly to CDFs (Fornara *et al.*, 2009), tissue specificity is important for *FLORE* function (Fig. S4c).

Thirdly, we evaluated the role of the siRNA biogenesis pathway (*dcl3-1*, *dcl2dcl4*) or the *trans*-acting *ta*-siRNA pathway (*drb4-2*) in regulating *FLORE* and *CDF5* circadian waving patterns. Under 12L/D conditions we confirmed the antiphasic circadian waveforms of both NAT pair components that remained mostly unaltered in these mutants, although we detected higher levels of *FLORE* transcripts during the dark period (ZT18-ZT21) in *dcl2dcl4* mutants (Fig. S5). We investigated whether PolIV- and/or PolV-dependent siRNAs could promote DNA methylation, and consequently transcriptional inhibition at the *CDF5/FLORE locus*. We initially analysed the available DNA methylomes of 86 *Arabidopsis* gene silencing mutants which revealed that either CG, CHG or CHH methylation were not highly accumulated (CG) or almost absent (CHG, CHH) in both strands at this *locus* (Stroud *et al.*, 2013) (http://genomes.mcdb.ucla.edu/AthBSeq/). In addition we also confirmed the characteristic circadian antiphasic expression of *FLORE* and *CDF5* in *polIV*, *polV* and *ddc* mutants grown under 12 L/D conditions (Fig. S6).

Fourthly, we determined the exact amounts of *FLORE* and *CDF5* transcripts both at their peak and trough times (ZT0, ZT12) under 12L/D conditions using a qPCR-based approach with fragment-specific calibration curves. In WT, *FLORE* transcript levels increased approximately 10-fold from ZT0 to ZT12; oppositely, *CDF5* transcript levels decreased approximately 10-fold from ZT0 to ZT12. *FLORE* and *CDF5* transcript levels also showed daily dynamics; in the early morning there was a 86.6-fold excess of *CDF5* in relation to *FLORE*. However at ZT12, *CDF5* transcript accumulation decreased and mirrored *FLORE* transcript levels which had increased during the day (Fig. S7). At ZT0 the majority of the mutants evaluated did not show any relevant changes (above 2-fold) in both *CDF5/FLORE* expression; with the exception of *dcl3-1*, *dcl2dcl4* and *polIV* where the increase in *FLORE* transcript levels was close to 2-fold. At ZT12 however, this regulation of transcript levels varied in the different mutants. The equal amount relationship seen in WT was still somewhat maintained in *drb4-2*, *ddc*, and *polV* mutants. However, in the other mutants there was either a 2-fold increase in *FLORE* transcript levels (*dcl3-1*) or a 2-3 fold reduction in *CDF5* transcript levels [*dcl2dcl4*, *polIV* and *rna-dependent rna polymerase2-1* (*rdr2-1* (Xie *et al.*, 2004)), respectively]. These differences, however, were not reflected in significant changes in *FLORE* and *CDF5* circadian expression patterns. Our findings suggest that the mutual repression between *FLORE* and *CDF5* is most likely independent of small RNA pathways, indicating that other mechanisms could be at play.

Discussion

The identification and functional characterization of lncRNAs has shed light on the relevance of the noncoding transcriptome for the survival and fitness of whole organisms. Despite its relatively small size, only 50% of the *Arabidopsis* genome encodes protein-coding transcripts (Ariel *et al.*, 2015). In addition, 70% of the annotated *Arabidopsis* mRNAs are associated with antisense transcripts, many of which are lncRNAs (Wang, H *et al.*, 2014). We identified the lncRNA *FLORE*, which is expressed antisense to the *CDF5* transcript. Moreover, *FLORE* circadian oscillation pattern is antiphasic to *CDF5*. By modulating *FLORE* transcript levels, either by T-DNA insertion mutagenesis or tissue-specific overexpression, we found that this anti-parallel behaviour reflected a mutual inhibitory relationship (Fig.6). Furthermore, we observed that *FLORE* could function not only in *cis* affecting *CDF5,* but also in *trans* by regulating other *CDF*s such as *CDF1* and *CDF3*.

FLORE, similarly to *CDF5*, is a *bona fide* circadian-regulated transcript that maintained its oscillation pattern of expression under all the conditions tested, except in circadian-affected transgenic lines grown under LL conditions (e.g. *CCA1*-overexpressors; Fig. 1). Moreover, *FLORE* has also been identified as a direct target of PRR7 (PSEUDO RESPONSE REGULATOR 7), a core clock component (Liu *et al.*, 2013). Although circadian-regulated lncRNAs have been reported both in plants and animals (Hazen *et al.*, 2009; Coon *et al.*, 2012; Xue *et al.*, 2014), their precise mechanisms of action are mostly unknown. In the fungus *Neurospora*, however, the circadian oscillator component *frequency* (*frq*) and its lncRNA *qrf* constitute a NAT pair with an antiphasic pattern of expression that also reflects a mutual inhibitory relationship (Xue *et al.*, 2014). This opposite behaviour is critical for the maintenance of robust circadian oscillation of *frq* and *qrf*, as well as proper circadian feedback loops in the *Neurospora* clock. Similar to *frq* and *qrf*, *FLORE* and *CDF5* display an antiphasic expression pattern that depends on their dynamic relationship. We showed that, in the absence of endogenous *CDF5*, *FLORE*-promoter driven *CDF5* expression affected not only *CDF5* transcript levels, but also the amplitude of *FLORE* oscillation (Fig. 4).
Considering that *FLORE* (Fig. 3b) and *CDF5* (Fornara *et al.*, 2009) are vascular tissue-specific transcripts, we propose that the circadian clock regulates their oscillatory expression (e.g. by core clock components such as PRR7), which is then maintained and reinforced by their mutual inhibition (Fig. 6). NATs have also been described for the mammal core clock component *Period* (Vollmers *et al.*, 2012; Li *et al.*, 2015), indicating that antisense transcription could play a relevant role in fine-tuning circadian gene expression. Most likely this regulation encompasses central oscillator components (*frq*/*qrf* and *Period*) and circadian output transcripts (*CDF5*/*FLORE*). Our results further suggest that *FLORE* could not only contribute to the robustness of *CDF5* oscillation but also modulate the expression patterns of other *CDF*s (e.g. *CDF1* and *CDF3*), and thus contribute to their precise diurnal accumulation. On the other hand, *CDF5* and possibly other *CDF*s (*CDF1*, *CDF2* and *CDF3*) would act as negative regulators of *FLORE* expression (Fig. 2d; Fig. 6).

The reciprocal inhibition between *FLORE* and *CDF5* transcripts is also reflected in opposite biological function. Whereas *CDF5* transcript accumulation delayed flowering (Fornara *et al.*, 2009), *FLORE* transcript enrichment promoted it, both under LD and SD conditions (Fig. 5; Fig. S2). *CDF5*, similarly to the other *CDF*s, is under circadian transcriptional and post-translational control and this regulatory mechanism constitutes a molecular link between the circadian clock and photoperiodic-dependent flowering (Imaizumi *et al.*, 2005; Sawa *et al.*, 2007; Fornara *et al.*, 2009; Song *et al.*, 2015). *CDF5* expression is directly controlled by the central oscillator components PRR5, PRR7 and PRR9 (Nakamichi *et al.*, 2012; Liu *et al.*, 2013), while CDF5 protein levels are most likely regulated by the F-box protein FKF1 (FLAVIN-BINDING, KELCH REPEAT, F-BOX 1) and GI (GIGANTEA). The coordinated association of FKF1 and GI would then promote CDF5 ubiquitination and degradation by proteasomes (Sawa *et al.*, 2007). Under LD this regulatory mechanism promotes the accumulation of CO protein, *FT* expression and flowering (Imaizumi *et al.*, 2005; Sawa *et al.*, 2007). Our findings suggest an additional step in this process that includes the lncRNA *FLORE*. We could show that vascular accumulation of *FLORE* promoted flowering and this correlated with an increase in *CO* expression and higher accumulation of *FT* transcripts (Fig. 5; Fig. S2). This up-regulation of *FT* is probably due to the dual effect on its transcription, resulting from the depletion in its repressors (CDFs) and accumulation of its activator (CO). Our analysis of *cdf-q* mutants also confirmed the differential effect of *CDF*s in *CO* and *FT* expression (Notes S3). A similar correlation has also been reported in *Chlamydomonas reinhardtii* overexpressing *CrDOF* (the sole *CDF* homolog) where a small inhibition in *CO* promoted a strong decrease in *FT* expression (Lucas-Reina *et al.*, 2015). Confirming previous reports (Imaizumi *et al.*, 2005; Fornara *et al.*, 2009), we observed that overexpression approaches resulted in stronger phenotypic responses than T-DNA insertion mutagenesis. We attribute these results to the high degree of functional redundancy within the *CDF* family, where the decrease in one *CDF* transcript could be compensated by other family members. Nevertheless, collectively our results suggest that *CDF5* and *FLORE* biological role would rely on their antiphasic expression pattern and reciprocal inhibition.

This mutual regulation could be explained by several mechanisms. For instance, similar to other NAT pairs, *CDF5/FLORE* transcripts could form long dsRNAs that would generate nat-siRNAs due to processing by DCL (DICER LIKE) (Zubko & Meyer, 2007;

Held *et al.*, 2008; Ma *et al.*, 2014). Moreover, because of sequence homology some of these nat-siRNAs could also trigger RNA-dependent DNA methylation (RdDM) of the *FLORE* and/or *CDF5 locus* resulting in transcriptional inhibition. However, although we detected some variation in *FLORE* and/or *CDF5* transcript levels in some of the siRNA biogenesis or RdDM machinery mutants grown under 12 L/D conditions, these changes were not higher than 2-3 fold and did not affect the typical antiphasic expression pattern of this NAT pair (Fig. S5 and Fig. S6). In addition, siRNAs were not detected in WT plants (Fig. S4). Furthermore, constitutive ectopic expression of *FLORE*, and consequent siRNA accumulation, did not produce a clear flowering phenotype (Fig. S4). We also analysed the small RNAs generated by this *locus*, and siRNA accumulation leading to DNA methylation (Stroud *et al.*, 2013), but failed to find any relevant accumulation of either smRNAs or CG, CHH or CHG methylation in the *CDF5/FLORE locus*. Taken together these results led us to hypothesize that siRNA generation and accompanying gene silencing would not be the preferential mechanism underlying the *CDF5/FLORE* mutual inhibition.

In fact, although siRNA generation was initially proposed as the main mechanism underlying NAT-lncRNA function, mounting evidence suggests a wider landscape of regulatory roles (Bazin & Bailey-Serres, 2015). Possible mechanisms could include the recruitment of chromatin modifiers and induction of epigenetic changes under particular environmental conditions (Swiezewski *et al.*, 2009; Heo & Sung, 2011; Ietswaart *et al.*, 2012; Jones & Sung, 2014; Rosa *et al.*, 2016). Pol II stalling and the accumulation of truncated dysfunctional RNAs due to convergent transcription (Xue *et al.*, 2014) could also occur, although this would preferably account for transcriptional regulation of *cis*-NATs. Since our results indicate that *FLORE* most likely acts in *cis* and *trans*, its function could rely on different strategies such as the modulation of chromatin dynamics and reshaping of nuclear organization similarly to *Xist* (*X-Inactive Specific Transcript*) or *Firre* (*Functional Intergenic Repeating RNA Element*) (Lee, 2012; Engreitz *et al.*, 2013; Simon *et al.*, 2013; Bergmann & Spector, 2014; Rinn & Guttman, 2014). Considering the ability of RNA to bind nucleic acids and proteins, *FLORE* could also interact with hitherto unknown RNA-binding proteins (X in Fig. 6) and thus modulate *CDF5* expression. Another possibility would be that *FLORE* modulates *CDF5* amounts also at the translational level, and this could be achieved by direct interaction with the translational machinery as was shown for the rice cis $NAT_{PHO1;2}$ (Jabnoune *et al.*, 2013).

On the other hand, CDF5 could also be a transcriptional regulator of *FLORE* (Fig. 6). Future studies are clearly needed to identify details of the molecular mechanism underlying this antiphasic regulation.

The perception and consequent response to day length seems to have evolved very early in plant evolution since it would allow physiological processes to track seasonal variability. These responses have thus evolved into a complex pathway that translates environmental and developmental cues into the appropriate timing for flowering, which we now propose to also include the long non-coding RNA *FLORE*. The identification of *CDF* homologs in the unicellular green algae *Chlamydomonas reinhardtii* (Lucas-Reina *et al.*, 2015) highlights the conservation of these DOF family members. In addition, our database searches uncovered putative *CDF*/*lncCDF* NAT pairs in other species (e.g. *Brassica napus* and *Medicago truncatula*), suggesting also evolutionary conservation of this regulatory module. Furthermore, CDFs have recently been implicated in regulating other biological processes such as abiotic stress responses, indicating a broader biological role for the *CDF5*/*FLORE* NAT pair in *Arabidopsis* (Fornara *et al.*, 2009; Corrales *et al.*, 2014; Fornara *et al.*, 2015; Corrales *et al.*, 2017). Considering a sequence homology-based function, *FLORE* could also regulate other *DOFs*, and the *CDF5/FLORE* module could be part of a regulatory pathway involved in other fundamental plant life cycle events.

Acknowledgements

The authors are grateful to Dr Paula Suaréz-Lopez and Dr Elena Monte for their useful comments and critical reading of the manuscript. This work has been funded in part by the European Commission (PCIG2012-GA-2012-334052) and by the MINECO (BIO2015-70812-ERC) to the laboratory of RH. JL is funded by the Agricultural Science and Technology Innovation Program of CAAS. We acknowledge the financial support to the CRAG from the CERCA programme / Generalitat de Catalunya and by the MINECO through the "Severo Ochoa Programme for Centers of Excellence in R&D" 2016-2019 (SEV-2015-0533)".

Author contribution

R.H. and N-H. C. designed the experiments. R.H., L-F. H. and M.B. performed the molecular and biochemical experiments. H.W. and J.L. designed the custom-array and performed all the bioinformatics analysis. R.H., J.L., H.W. and N-H. Chua discussed results and wrote the manuscript.

References

Ariel F, Jegu T, Latrasse D, Romero-Barrios N, Christ A, Benhamed M, Crespi M. 2014. Noncoding transcription by alternative RNA polymerases dynamically regulates an auxin-driven chromatin loop. *Molecular Cell* **55**(3): 383-396.

Ariel F, Romero-Barrios N, Jégu T, Benhamed M, Crespi M. 2015. Battles and hijacks: noncoding transcription in plants. *Trends in Plant Science* **20**(6): 362-371.

Bardou F, Ariel F, Simpson CG, Romero-Barrios N, Laporte P, Balzergue S, Brown JWS, Crespi M. 2014. Long noncoding RNA modulates alternative splicing regulators in *Arabidopsis*. *Developmental Cell* **30**(2): 166-176.

Bazin J, Bailey-Serres J. 2015. Emerging roles of long non-coding RNA in root developmental plasticity and regulation of phosphate homeostasis. *Frontiers in Plant Science* **6**: 400.

Bergmann JH, Spector DL. 2014. Long non-coding RNAs: modulators of nuclear structure and function. *Current Opinion in Cell Biology* **26**: 10-18.

Cao X, Aufsatz W, Zilberman D, Mette MF, Huang MS, Matzke M, Jacobsen SE. 2003. Role of the DRM and CMT3 methyltransferases in RNA-directed DNA methylation. *Current Biology* **13**(24): 2212-2217.

Coon SL, Munson PJ, Cherukuri PF, Sugden D, Rath MF, Müller M, Clokie SJH, Fu C, Olanich ME, Rangel Z, et al. 2012. Circadian changes in long noncoding RNAs in the pineal gland. *Proceedings of the National Academy of Sciences* **109**(33): 13319-13324.

Corrales A-R, Carrillo L, Lasierra P, Nebauer SG, Dominguez-Figueroa J, Renau-Morata B, Pollmann S, Granell A, Molina R-V, Vicente-Carbajosa J, et al. 2017. Multifaceted Role of *Cycling Dof Factor 3* (*CDF3*) in the regulation of flowering time and abiotic stress responses in *Arabidopsis*. *Plant, Cell & Environment* **40**(5): 748-764.

Corrales A-R, Nebauer SG, Carrillo L, Fernández-Nohales P, Marqués J, Renau-Morata B, Granell A, Pollmann S, Vicente-Carbajosa J, Molina R-V, et al. 2014. Characterization of tomato Cycling Dof Factors reveals conserved and new functions in the control of flowering time and abiotic stress responses. *Journal of Experimental Botany* **65**(4): 995-1012.

Csorba T, Questa JI, Sun Q, Dean C. 2014. Antisense *COOLAIR* mediates the coordinated switching of chromatin states at *FLC* during vernalization. *Proceedings of the National Academy of Sciences* **111**(45): 16160-16165.

Dodd A, Salathia N, Hall A, Kevei E, Toth R, Nagy F, Hibberd J, Millar A, Webb A. 2005. Plant circadian clocks increase photosynthesis, growth, survival, and competitive advantage. *Science* **309**(5734): 630-633.

Doherty CJ, Kay SA. 2010. Circadian control of global gene expression patterns. *Annu. Rev. Genet.* **44**(1): 419-444.

Engreitz JM, Pandya-Jones A, McDonel P, Shishkin A, Sirokman K, Surka C, Kadri S, Xing J, Goren A, Lander ES, et al. 2013. The *Xist* lncRNA exploits three-dimensional genome architecture to spread across the X chromosome. *Science* **341**(6147): 1237973.

Fatica A, Bozzoni I. 2014. Long non-coding RNAs: new players in cell differentiation and development. *Nat Rev Genet* **15**(1): 7-21.

Foo M, Somers DE, Kim P-J. 2016. Kernel architecture of the genetic circuitry of the *Arabidopsis* circadian system. *PLoS Comput Biol* **12**(2): e1004748.

Fornara F, de Montaigu A, Sánchez-Villarreal A, Takahashi Y, van Themaat EVL, Huettel B, Davis SJ, Coupland G. 2015. The GI-CDF module of *Arabidopsis* affects freezing tolerance and growth as well as flowering. *The Plant Journal* **81**(5): 695-706.

Fornara F, Panigrahi KCS, Gissot L, Sauerbrunn N, Rühl M, Jarillo JA, Coupland G. 2009. *Arabidopsis* DOF transcription factors act redundantly to reduce *CONSTANS* expression and are essential for a photoperiodic flowering response. *Developmental Cell* **17**(1): 75-86.

Franco-Zorrilla JM, Valli A, Todesco M, Mateos I, Puga MI, Rubio-Somoza I, Leyva A, Weigel D, Garcia JA, Paz-Ares J. 2007. Target mimicry provides a new mechanism for regulation of microRNA activity. *Nat Genet* **39**(8): 1033-1037.

Ha M, Kim VN. 2014. Regulation of microRNA biogenesis. *Nat Rev Mol Cell Biol* **15**(8): 509-524.

Hazen S, Naef F, Quisel T, Gendron J, Chen H, Ecker J, Borevitz J, Kay S. 2009. Exploring the transcriptional landscape of plant circadian rhythms using genome tiling arrays. *Genome Biol.* **10**(2): R17.

Held MA, Penning B, Brandt AS, Kessans SA, Yong W, Scofield SR, Carpita NC. 2008. Small-interfering RNAs from natural antisense transcripts derived from a cellulose synthase gene modulate cell wall biosynthesis in barley. *Proceedings of the National Academy of Sciences* **105**(51): 20534-20539.

Hemmes H, Henriques R, Jang I-C, Kim S, Chua N-H. 2012. Circadian clock regulates dynamic chromatin modifications associated with *Arabidopsis CCA1/LHY* and *TOC1* transcriptional rhythms. *Plant and Cell Physiology* **53**(12): 2016-2029.

Heo JB, Sung S. 2011. Vernalization-mediated epigenetic silencing by a Long Intronic Noncoding RNA. *Science* **331**(6013): 76-79.

Hsu PY, Calviello L, Wu H-YL, Li F-W, Rothfels CJ, Ohler U, Benfey PN. 2016. Super-resolution ribosome profiling reveals unannotated translation events in *Arabidopsis*. *Proceedings of the National Academy of Sciences* **113**(45): E7126-E7135.

Hughes ME, Hogenesch JB, Kornacker K. 2010. JTK_CYCLE: an efficient nonparametric algorithm for detecting rhythmic components in genome-scale data sets. *Journal of Biological Rhythms* **25**(5): 372-380.

Ietswaart R, Wu Z, Dean C. 2012. Flowering time control: another window to the connection between antisense RNA and chromatin. *Trends in Genetics* **28**(9): 445-453.

Imaizumi T, Schultz TF, Harmon FG, Ho LA, Kay SA. 2005. FKF1 F-Box protein mediates cyclic degradation of a repressor of *CONSTANS* in *Arabidopsis*. *Science* **309**(5732): 293-297.

Imlau A, Truernit E, Sauer N. 1999. Cell-to-cell and long-distance trafficking of the green fluorescent protein in the phloem and symplastic unloading of the protein into sink tissues. *The Plant Cell* **11**(3): 309-322.

Jabnoune M, Secco D, Lecampion C, Robaglia C, Shu Q, Poirier Y. 2013. A rice *cis*-natural antisense RNA acts as a translational enhancer for its cognate mRNA and contributes to phosphate homeostasis and plant fitness. *The Plant Cell* **25**(10): 4166-4182.

Jakubiec A, Yang SW, Chua N-H. 2012. *Arabidopsis* DRB4 protein in antiviral defense against Turnip yellow mosaic virus infection. *The Plant Journal* **69**(1): 14-25.

Jones AL, Sung S. 2014. Mechanisms underlying epigenetic regulation in *Arabidopsis thaliana*. *Integrative and Comparative Biology* **54**(1): 61-67.

Kanno T, Huettel B, Mette MF, Aufsatz W, Jaligot E, Daxinger L, Kreil DP, Matzke M, Matzke AJ. 2005. Atypical RNA polymerase subunits required for RNA-directed DNA methylation. *Nature Genetics* **37**: 761-765.

Karimi M, Inze D, Depicker A. 2002. GATEWAY$^{(TM)}$ vectors for *Agrobacterium*-mediated plant transformation. *Trends in Plant Science* **7**(5): 193-195.

Kiba T, Henriques R 2016. Assessing protein stability under different light and circadian conditions. In: Duque P ed. *Environmental Responses in Plants: Methods and Protocols*. New York, NY: Springer New York, 141-152.

Kiba T, Henriques R, Sakakibara H, Chua N. 2007. Targeted degradation of PSEUDO-RESPONSE REGULATOR5 by an SCF^{ZTL} complex regulates clock function and photomorphogenesis in *Arabidopsis thaliana*. *Plant Cell* **19**(8): 2516-2530.

Kim D-H, Sung S. 2017. Vernalization-triggered intragenic chromatin loop formation by Long Noncoding RNAs. *Developmental Cell* **40**(3): 302-312.

Kong L, Zhang Y, Ye Z-Q, Liu X-Q, Zhao S-Q, Wei L, Gao G. 2007. CPC: assess the protein-coding potential of transcripts using sequence features and support vector machine. *Nucleic Acids Research* **35**(suppl 2): W345-W349.

Kramer C, Loros JJ, Dunlap JC, Crosthwaite SK. 2003. Role for antisense RNA in regulating circadian clock function in *Neurospora crassa*. *Nature* **421**(6926): 948-952.

Krzymuski M, Andrés F, Cagnola JI, Jang S, Yanovsky MJ, Coupland G, Casal JJ. 2015. The dynamics of *FLOWERING LOCUS T* expression encodes long-day information. *The Plant Journal* **83**(6): 952-961.

Le Hir R, Bellini C. 2013. The plant-specific Dof transcription factors family: new players involved in vascular system development and functioning in *Arabidopsis*. *Frontiers in Plant Science* **4**: 164.

Lee JT. 2012. Epigenetic regulation by Long Noncoding RNAs. *Science* **338**(6113): 1435-1439.

Li N, Joska TM, Ruesch CE, Coster SJ, Belden WJ. 2015. The *frequency* natural antisense transcript first promotes, then represses, *frequency* gene expression via facultative heterochromatin. *Proceedings of the National Academy of Sciences* **112**(14): 4357-4362.

Liu J, Jung C, Xu J, Wang H, Deng S, Bernad L, Arenas-Huertero C, Chua N-H. 2012. Genome-wide analysis uncovers regulation of Long Intergenic Noncoding RNAs in *Arabidopsis*. *Plant Cell* **24**(11): 4333-4345.

Liu T, Carlsson J, Takeuchi T, Newton L, Farré EM. 2013. Direct regulation of abiotic responses by the *Arabidopsis* circadian clock component PRR7. *The Plant Journal* **76**(1): 101-114.

Lucas-Reina E, Romero-Campero FJ, Romero JM, Valverde F. 2015. An evolutionarily conserved DOF-CONSTANS module controls plant photoperiodic signaling. *Plant Physiology* **168**(2): 561-574.

Luo C, Sidote DJ, Zhang Y, Kerstetter RA, Michael TP, Lam E. 2013. Integrative analysis of chromatin states in *Arabidopsis* identified potential regulatory mechanisms for natural antisense transcript production. *The Plant Journal* **73**(1): 77-90.

Ma X, Shao C, Jin Y, Wang H, Meng Y. 2014. Long non-coding RNAs: A novel endogenous source for the generation of Dicer-like 1-dependent small RNAs in *Arabidopsis thaliana*. *RNA Biology* **11**(4): 23-22.

Magistri M, Faghihi MA, St Laurent III G, Wahlestedt C. 2012. Regulation of chromatin structure by long noncoding RNAs: focus on natural antisense transcripts. *Trends in Genetics* **28**(8): 389-396.

Malapeira J, Khaitova LC, Mas P. 2012. Ordered changes in histone modifications at the core of the *Arabidopsis* circadian clock. *Proc Natl Acad Sci U S A* **109**(52): 21540-21545.

Mi S, Cai T, Hu Y, Chen Y, Hodges E, Ni F, Wu L, Li S, Zhou H, Long C, et al. 2008. Sorting of small RNAs into *Arabidopsis* Argonaute complexes is directed by the 5' terminal nucleotide. *Cell* **133**(1): 116-127.

Montgomery TA, Howell MD, Cuperus JT, Li D, Hansen JE, Alexander AL, Chapman EJ, Fahlgren N, Allen E, Carrington JC. 2008. Specificity of ARGONAUTE7-miR390 Interaction and Dual Functionality in *TAS3 Trans*-Acting siRNA Formation. *Cell* **133**(1): 128-141.

Nakamichi N, Kiba T, Kamioka M, Suzuki T, Yamashino T, Higashiyama T, Sakakibara H, Mizuno T. 2012. Transcriptional repressor PRR5 directly regulates clock-output pathways. *Proceedings of the National Academy of Sciences* **109**(42): 17123-17128.

Onodera Y, Haag JR, Ream T, Nunes PC, Pontes O, Pikaard CS. 2005. Plant nuclear RNA polymerase IV mediates siRNA and DNA methylation-dependent heterochromatin formation. *Cell* **120**(5): 613-622.

Osnato M, Castillejo C, Matías-Hernández L, Pelaz S. 2012. *TEMPRANILLO* genes link photoperiod and gibberellin pathways to control flowering in Arabidopsis. *Nat Commun* **3**: 808.

Rinn J, Guttman M. 2014. RNA and dynamic nuclear organization. *Science* **345**(6202): 1240-1241.

Rosa S, Duncan S, Dean C. 2016. Mutually exclusive sense-antisense transcription at *FLC* facilitates environmentally induced gene repression. *Nature Communications* **7**: 13031.

Sabin LR, Delás MJ, Hannon GJ. 2013. Dogma Derailed: The many influences of RNA on the genome. *Molecular Cell* **49**(5): 783-794.

Sawa M, Nusinow DA, Kay SA, Imaizumi T. 2007. FKF1 and GIGANTEA complex formation is required for day-length measurement in *Arabidopsis*. *Science* **318**(5848): 261-265.

Shafiq S, Li J, Sun Q. 2016. Functions of plants long non-coding RNAs. *Biochimica et Biophysica Acta (BBA) - Gene Regulatory Mechanisms* **1859**(1): 155-162.

Simon MD, Pinter SF, Fang R, Sarma K, Rutenberg-Schoenberg M, Bowman SK, Kesner BA, Maier VK, Kingston RE, Lee JT. 2013. High-resolution *Xist* binding maps reveal two-step spreading during X-chromosome inactivation. *Nature* **504**(7480): 465-469.

Song H-R, Noh Y-S. 2012. Rhythmic oscillation of histone acetylation and methylation at the *Arabidopsis* central clock loci. *Molecules and Cells* **34**(3): 279-287.

Song J, Angel A, Howard M, Dean C. 2012. Vernalization - a cold-induced epigenetic switch. *Journal of Cell Science* **125**(16): 3723-3731.

Song YH, Shim JS, Kinmonth-Schultz HA, Imaizumi T. 2015. Photoperiodic flowering: time measurement mechanisms in leaves. *Annual Review of Plant Biology* **66**(1): 441-464.

Song YH, Smith RW, To BJ, Millar AJ, Imaizumi T. 2012. FKF1 conveys timing information for CONSTANS stabilization in photoperiodic flowering. *Science* **336**(6084): 1045-1049.

Stroud H, Greenberg MVC, Feng S, Bernatavichute YV, Jacobsen SE. 2013. Comprehensive analysis of silencing mutants reveals complex regulation of the *Arabidopsis* methylome. *Cell* **152**(1-2): 352-364.

Swiezewski S, Liu F, Magusin A, Dean C. 2009. Cold-induced silencing by long antisense transcripts of an *Arabidopsis* Polycomb target. *Nature* **462**(7274): 799-802.

Vollmers C, Schmitz RJ, Nathanson J, Yeo G, Ecker JR, Panda S. 2012. Circadian oscillations of protein-coding and regulatory RNAs in a highly dynamic mammalian liver epigenome. *Cell Metabolism* **16**(6): 833-845.

Wang H, Chung PJ, Liu J, Jang I-C, Kean MJ, Xu J, Chua N-H. 2014. Genome-wide identification of long noncoding natural antisense transcripts and their responses to light in *Arabidopsis*. *Genome Research* **24**(3): 444-453.

Wang Y, Fan X, Lin F, He G, Terzaghi W, Zhu D, Deng XW. 2014. *Arabidopsis* noncoding RNA mediates control of photomorphogenesis by red light. *Proceedings of the National Academy of Sciences* **111**(28): 10359-10364.

Xie Z, Allen E, Wilken A, Carrington JC. 2005. DICER-LIKE 4 functions in *trans*-acting small interfering RNA biogenesis and vegetative phase change in *Arabidopsis thaliana*. *Proc Natl Acad Sci U S A* **102**(36): 12984-12989.

Xie Z, Johansen LK, Gustafson AM, Kasschau KD, Lellis AD, Zilberman D, Jacobsen SE, Carrington JC. 2004. Genetic and functional diversification of small RNA pathways in plants. *PLoS biology*: 2, E104.

Xue Z, Ye Q, Anson SR, Yang J, Xiao G, Kowbel D, Glass NL, Crosthwaite SK, Liu Y. 2014. Transcriptional interference by antisense RNA is required for circadian clock function. *Nature* **514**(7524): 650-653.

Yanagisawa S. 2002. The Dof family of plant transcription factors. *Trends in Plant Science* **7**(12): 555-560.

Zhang X, Henriques R, Lin S-S, Niu Q-W, Chua N-H. 2006. *Agrobacterium*-mediated transformation of *Arabidopsis thaliana* using the floral dip method. *Nature Protocols* **1**(2): 641-646.

Zhang X, Lii Y, Wu Z, Polishko A, Zhang H, Chinnusamy V, Lonardi S, Zhu J-K, Liu R, Jin H. 2013. Mechanisms of small RNA generation from cis-NATs in response to environmental and developmental cues. *Molecular Plant* **6**(3): 704-715.

Zubko E, Meyer P. 2007. A natural antisense transcript of the *Petunia hybrida Sho* gene suggests a role for an antisense mechanism in cytokinin regulation. *The Plant Journal* **52**(6): 1131-1139.

Figure Legends

Figure 1. The natural antisense pair *CDF5* (*CYCLING DOF FACTOR 5*) / *FLORE* (*CDF5 LONG NON-CODING RNA*) antiphasic oscillation is regulated by the circadian clock in *Arabidopsis*. (a) Schematics of the *CDF5*/*FLORE locus*. Yellow rectangle represents part of the *CDF5* promoter, orange rectangles depict *5'UTR* (*5'UnTranslated Region*) and *3'UTR* (*3'UnTranslated Region*), and the black lines are introns. Light green rectangle corresponds to part of the *FLORE* promoter, whereas red rectangles are *CDF5* exons and dark green rectangles are *FLORE* exons. (+) and (-) represent sense and antisense strands, respectively. *FLORE* (upper panels) and *CDF5* (lower panels) antiphasic circadian waveforms under short day **(b)**, 12 L/D **(c)**, long day **(d)** and continuous light conditions (LL) in WT Col-0 **(e)** and *CCA1* (*CIRCADIAN CLOCK ASSOCIATED 1*)-overexpressing seedlings **(f)** determined by qPCR (quantitative real time reverse transcription PCR) after normalizing with *Actin2* (At3g18780). Values shown are means ± SD (Standard Deviation) of three technical amplifications in one representative experiment out of three biological replicates. Primer pairs designed to evaluate *FLORE* transcript levels amplified the TAIR10 splicing variant, unless otherwise stated. Grey and dashed rectangles correspond to dark and subjective night periods, respectively. Time (h) represents the hours after lights on.

Figure 2. *Arabidopsis CDF5* (*CYCLING DOF FACTOR 5*) negatively regulates *FLORE* (*CDF5 LONG NON-CODING RNA*) transcript levels. (a) Schematics of T-DNA insertion events in the non-overlapping regions of the *CDF5 locus*. Orange rectangles represent *5'UTR* (*5'UnTranslated Region*) and *3'UTR* (*3'UnTranslated Region*) regions of *CDF5*, respectively. Red rectangles are exons and the black line represents the intron. **(b)** T-DNA insertion into the *CDF5* promoter results in a small decrease in *CDF5* transcript levels, while the *FLORE* waveform remains mostly similar to WT (Wild-Type). **(c)** Depletion of *CDF5* transcripts by a *5'UTR* T-DNA insertion leads to an increase in *FLORE* transcript levels. *CDF5* and *FLORE* transcript levels were

determined by qPCR (quantitative real time reverse-transcription PCR) after normalization with *Actin2*. Values shown are means ± SD (Standard Deviation) of three technical replicates from one representative experiment out of two biological duplicates analysed for each mutant allele. **(d)** Inhibition of *CDF1* (*CYCLING DOF FACTOR 1*), *CDF2* (*CYCLING DOF FACTOR 2*), *CDF3* (*CYCLING DOF FACTOR 3*) and *CDF5* expression in a *cdf-quadruple* mutant (*cdf-q*) promotes accumulation of *FLORE* transcripts throughout most of the day, whereas *CDF5* accumulation (*CDF5*-Ox) in the vasculature inhibits *FLORE* transcript levels. qPCR analysis was performed as described previously. Grey rectangles represent the dark period. Time (h) represents the hours after lights on.

Figure 3. *FLORE* (*CDF5 LONG NON-CODING RNA*) accumulates in the vasculature of *Arabidopsis* where it negatively regulates *CDF5* (*CYCLING DOF FACTOR 5*), *CDF1* (*CYCLING DOF FACTOR 1*) and *CDF3* (*CYCLING DOF FACTOR 3*) expression. Overexpression of *FLORE* driven by the *SUC2* vascular tissue specific promoter (*pSUC2*) leads to a reduction in amplitude of *CDF5* waveform as determined by qPCR (quantitative real time reverse-transcription PCR) normalized with respect to *Actin2* **(a)**. Values shown are means ± SD (Standard Deviation) of three technical triplicates from one representative experiment out of two biological duplicates evaluated. *FLORE* promoter-driven *GUS* reporter accumulates in the vascular tissue of 2 week-old seedlings **(b)** and flowers **(c)**. Two week-old seedlings expressing the empty vector control failed to show *GUS* accumulation **(d)**. Scale bars: 5mm in **(b)**, 1 mm in **(b)** inset detail, 1mm **(c)** and 2mm **(d)**. *CDF1* and *CDF3* circadian waveforms also show reduced amplitude in *pSUC2:FLORE* plants **(e)**. qPCR was performed as described above. Grey rectangles represent the dark period under long day conditions. Time (h) indicates the hours after lights on.

Figure 4. Time shifted expression of *CDF5* (*CYCLING DOF FACTOR 5*) affects *FLORE* (*CDF5 LONG NON-CODING RNA*) transcript levels in *Arabidopsis*. Schematics of cloning strategy **(a)**. *CDF5* was expressed from the *FLORE* promoter and this construct was introduced into the *cdf5-5'utr* mutant. Yellow rectangle represents part of the *CDF5* promoter, orange rectangles depict *5'UTR* (*5'UnTranslated Region*) and *3'UTR* (*3'UnTranslated Region*), and the black lines are introns. Light green rectangle corresponds to the *FLORE* promoter, whereas red rectangles are *CDF5* exons and dark

green rectangles are *FLORE* exons. (+) and (-) represent sense and antisense strands, respectively. Expression of *CDF5* under the control of the *FLORE* promoter in a *cdf5-5'utr* mutant results in *CDF5* transcript accumulation throughout the day **(b)** and the inhibition of the *FLORE* waveform **(c)**, as determined by qPCR (quantitative real time reverse-transcription PCR) normalized with *Actin2*. Results shown are the means ± SD (Standard Deviation) of three technical repeats in one representative experiment out of two biological replicates. Grey rectangles represent the dark period and Time (h) represents hours after lights on.

Figure 5. Modulation of *Arabidopsis CDF5* (*CYCLING DOF FACTOR 5*) and *FLORE* (*CDF5 LONG NON-CODING RNA*) transcript levels affects flowering under long days. (a) Depletion of *CDF5* transcript in the *cdf5-5'utr* mutant results in a slightly early flowering phenotype (Student's *t*-test, **P<0.05), measured in number of days (blue), rosette (green) and cauline leaves (yellow), in two biological replicates analysed (n=21). Each biological replicate included ten WT (Wild-Type, Col-0) plants, unless otherwise stated. **(b)** Modulation of *FLORE* transcript levels in *flore-prom* mutant plants grown under long day conditions alters flowering time determined by rosette leaf number (Student's *t*-test, ***P<0.001). Flowering time was evaluated by three parameters exactly as described above, in three independent experiments (n=47) with thirty-three WT plants as control. **(c, d)** *pSUC2*-driven overexpression of *FLORE* induces early flowering under long day conditions measured in number of days (blue), rosette leaf (green) and cauline leaf (yellow) number (Student's *t*-test ***P<0.0001). The flowering phenotype was visible as early as 19 days after transfer to long day conditions **(c)** and confirmed in two biological duplicates (n=24) **(d)**. The *cdf-q* mutant was used as a control for the early flowering phenotype. Scale bar 1 cm. qPCR (quantitative real time reverse-transcription PCR) analysis showed that this phenotype correlated with a higher increase in *FT* (*FLOWERING LOCUS T*) expression levels but with a smaller change in *CO* (*CONSTANS*) transcript accumulation **(e)**. qPCR results were normalized with respect to *Actin2* and presented as the mean ± SD (Standard Deviation) of three technical replicates in one representative experiment out of two biological duplicates analysed. **(f)** Expressing *CDF5* under the control of the *FLORE* promoter in a *cdf5-5'utr* mutant resulted in delayed flowering under long days evaluated as number of days (blue), rosette leaf (green) and cauline leaf (yellow) numbers (n=20) in a representative experiment out of two biological replicates where two independent lines were analysed (Student's *t*-test

P<0.05; *** P< 0.005). **(g) The delayed flowering phenotype was associated with a decrease in *FT* transcript levels as determined by qPCR. These results were analysed as described above. Grey rectangles represent the dark period and Time (h) indicates the hours after lights on.

Figure 6. Model of *CDF5* (*CYCLING DOF FACTOR 5*) and *FLORE* (*CDF5 LONG NON-CODING RNA*) mutual regulation in *Arabidopsis*. *CDF5* and *FLORE* constitute a circadian-regulated NAT (Natural Antisense Transcript) pair with an antiphasic pattern of expression. This is a consequence of mutual inhibition; *CDF5* inhibits *FLORE* accumulation in the afternoon, whereas *FLORE* represses *CDF5* in the morning. In addition, other *CDF*s [*CDF1* (*CYCLING DOF FACTOR 1*), *CDF2* (*CYCLING DOF FACTOR 2*), *CDF3* (*CYCLING DOF FACTOR 3*)] could repress *FLORE* both in the morning and afternoon (purple lines). On the other hand, *FLORE* could also act as their negative regulator. Both *CDF5* and *FLORE* transcripts accumulate in the vascular tissue where they oppositely regulate the *CO* (*CONSTANS*) - *FT* (*FLOWERING LOCUS T*) module and consequently flowering time. Straight-end lines depict repression, whereas green arrows indicate induction. The oscillation patterns of *CDF5* (red) and *FLORE* (green) are also depicted. Open questions in the model are marked with (?). Grey rectangle represents the dark period under LDs (Long Days).

Supporting Information

The following Supporting Information is available for this article.

Fig. S1 Description of the *FLORE*/*CDF5* NAT pair under short day conditions.

Fig. S2 *FLORE* vascular expression promotes early flowering both under long day and short day conditions.

Fig. S3 Modulation of *FLORE* transcripts affects *CDF*s.

Fig. S4 *FLORE* biological function requires tissue specificity and is mostly independent of siRNA accumulation.

Fig. S5 *FLORE* and *CDF5* expression patterns are conserved in plants affected in siRNA and ta-siRNA biogenesis.

Fig. S6 *FLORE* and *CDF5* waveforms are maintained in plants affected in the RdDM silencing pathway.

Fig. S7 *FLORE* and *CDF5* transcripts absolute amounts in mutants affected in siRNA or ta-siRNA biogenesis or the RdDM silencing pathway.

Table S1 Primers used for genotyping of *flore-prom*, *cdf5-prom* and *cdf5-5'utr* T-DNA insertion mutants.

Table S2 Primers used for cloning of *CDF5* and *FLORE* (genomic, cDNA and promoter sequences).

Table S3 Primers used for quantitative real-time RT-PCR (qPCR).

Methods S1 Hybridization protocol to profile lncRNA expression in *Arabidopsis*.

Methods S2 QPCR protocol using fragment specific standard curves.

Notes S1 List of oscillating circadian protein coding genes **(a)**, candidate long non-coding RNAs **(b)** and *FLORE* **(c)** identified in the screen of the ATH lincRNA v1 array (see separate file).

Notes S2 Results from biological duplicates of experiments shown in Fig. 1 and Fig. 5.

Notes S3 *CO* and *FT* transcript levels in *cdf-q* mutants described in Fig. 2d.

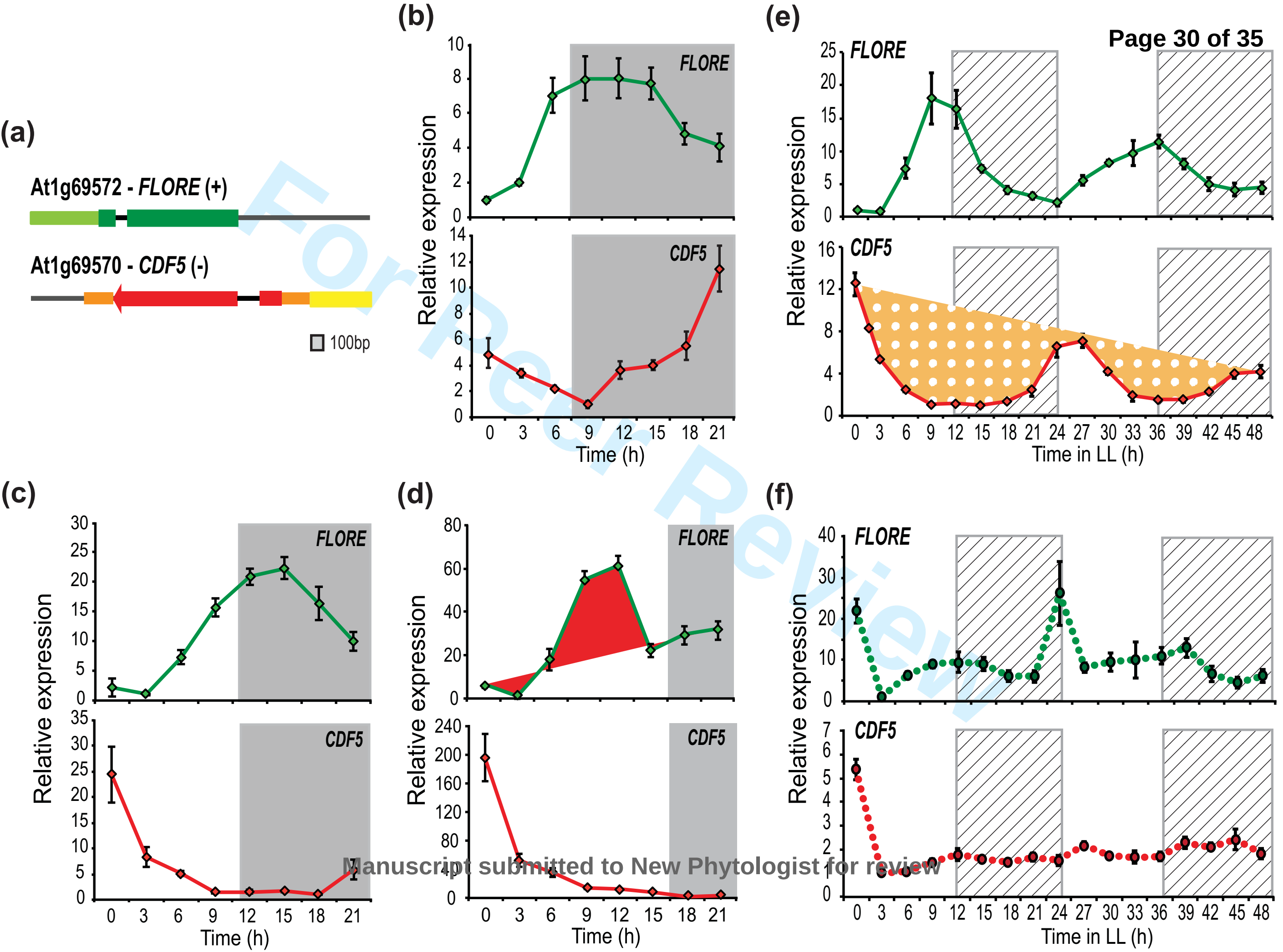
(a)
At1g69572 - FLORE (+)
At1g69570 - CDF5 (-)
100bp
(b)
FLORE
CDF5
Relative expression
Time (h)
(c)
FLORE
CDF5
Relative expression
Time (h)
(d)
FLORE
CDF5
Relative expression
Time (h)
(e)
FLORE
CDF5
Relative expression
Time in LL (h)
(f)
FLORE
CDF5
Relative expression
Time in LL (h)

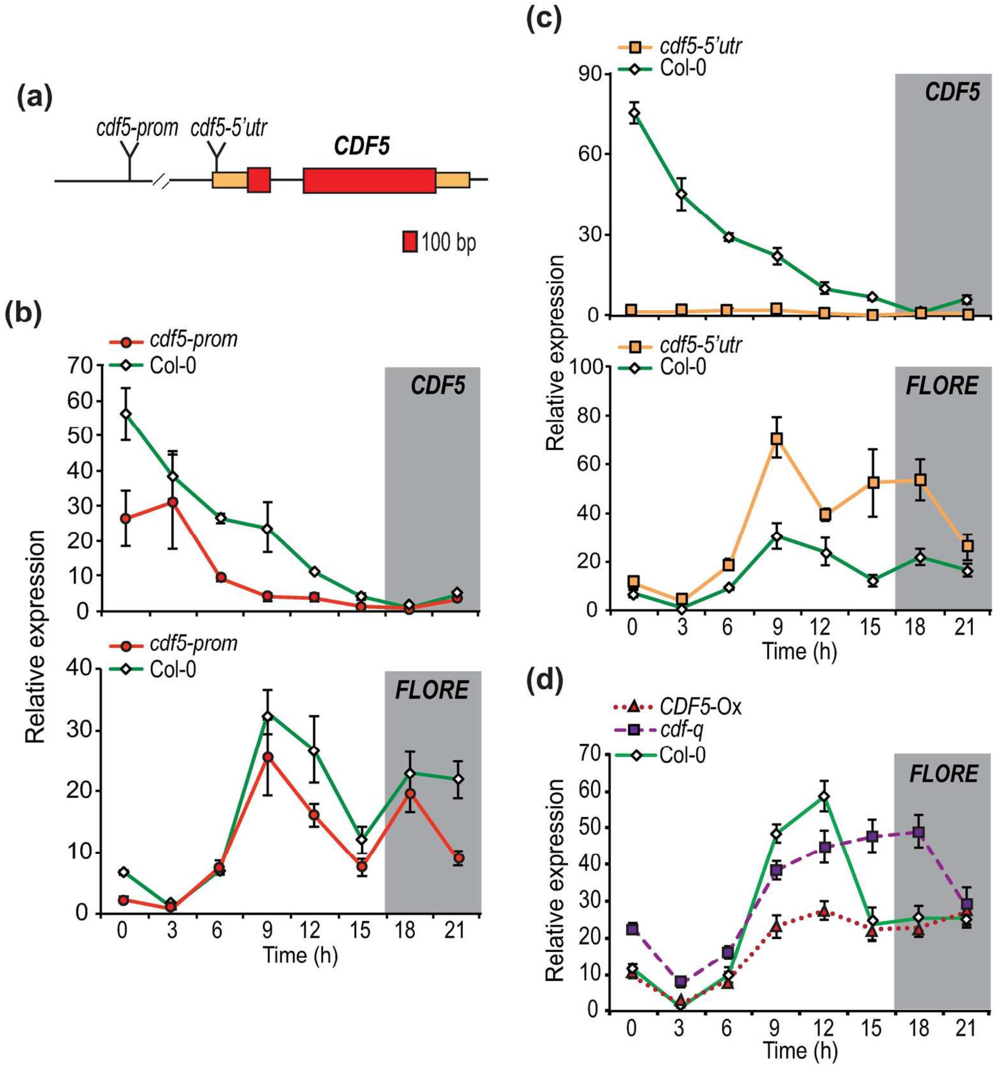

Figure 2. *Arabidopsis CDF5 (CYCLING DOF FACTOR 5)* negatively regulates *FLORE (CDF5 LONG NON-CODING RNA)* transcript levels. (a) Schematics of T-DNA insertion events in the non-overlapping regions of the *CDF5 locus*. Orange rectangles represent *5'UTR (5'UnTranslated Region)* and *3'UTR (3'UnTranslated Region)* regions of *CDF5*, respectively. Red rectangles are exons and the black line represents the intron. **(b)** T-DNA insertion into the *CDF5* promoter results in a small decrease in *CDF5* transcript levels, while the *FLORE* waveform remains mostly similar to WT (Wild-Type). **(c)** Depletion of *CDF5* transcripts by a *5'UTR* T-DNA insertion leads to an increase in *FLORE* transcript levels. *CDF5* and *FLORE* transcript levels were determined by qPCR (quantitative real time reverse-transcription PCR) after normalization with *Actin2*. Values shown are means ± SD (Standard Deviation) of three technical replicates from one representative experiment out of two biological duplicates analysed for each mutant allele. **(d)** Inhibition of *CDF1 (CYCLING DOF FACTOR 1)*, *CDF2 (CYCLING DOF FACTOR 2)*, *CDF3 (CYCLING DOF FACTOR 3)* and *CDF5* expression in a *cdf-quadruple* mutant (*cdf-q*) promotes accumulation of *FLORE* transcripts throughout most of the day, whereas *CDF5* accumulation (*CDF5*-Ox) in the vasculature inhibits *FLORE* transcript levels. qPCR analysis was performed as described previously. Grey rectangles represent the dark period. Time (h) represents the hours after lights on.

173x184mm (300 x 300 DPI)

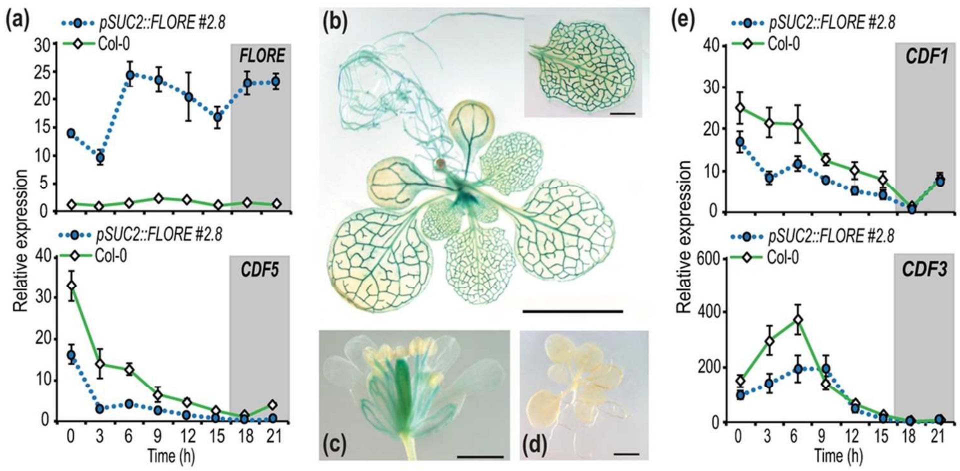

Figure 3. *FLORE (CDF5 LONG NON-CODING RNA)* accumulates in the vasculature where it negatively regulates *CDF5 (CYCLING DOF FACTOR 5)*, *CDF1 (CYCLING DOF FACTOR 1)* and *CDF3 (CYCLING DOF FACTOR 3)*expression. Overexpression of *FLORE* driven by the *SUC2* vascular tissue specific promoter (*pSUC2*) leads to a reduction in amplitude of *CDF5* waveform as determined by qPCR (quantitative real time reverse-transcription PCR) normalized with respect to *Actin2* **(a)**. Values shown are means ± SD (Standard Deviation) of three technical triplicates from one representative experiment out of two biological duplicates evaluated. *FLORE* promoter-driven *GUS* reporter accumulates in the vascular tissue of 2 week-old seedlings **(b)** and flowers **(c)**. Two week-old seedlings expressing the empty vector control failed to show *GUS* accumulation **(d)**. Scale bars: 5mm in **(b)**, 1 mm in **(b)** inset detail, 1mm **(c)** and 2mm **(d)**. *CDF1* and *CDF3* circadian waveforms also show reduced amplitude in *pSUC2:FLORE* plants **(e)**. qPCR was performed as described above. Grey rectangles represent the dark period under long day conditions. Time (h) indicates the hours after lights on.

99x50mm (300 x 300 DPI)

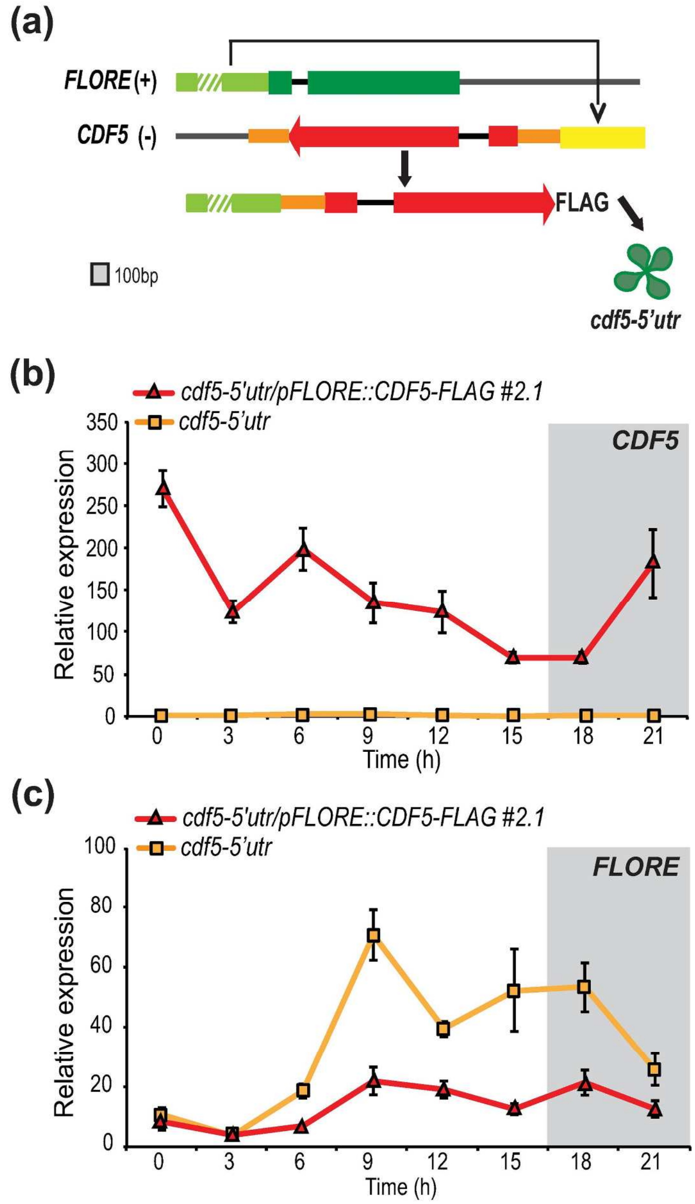

Figure 4. Time shifted expression of *CDF5 (CYCLING DOF FACTOR 5)* affects *FLORE (CDF5 LONG NON-CODING RNA)* transcript levels in *Arabidopsis*. Schematics of cloning strategy **(a)**. *CDF5* was expressed from the *FLORE* promoter and this construct was introduced into the *cdf5-5'utr* mutant. Yellow rectangle represents part of the *CDF5* promoter, orange rectangles depict *5'UTR (5'UnTranslated Region)* and *3'UTR (3'UnTranslated Region)*, and the black lines are introns. Light green rectangle corresponds to the *FLORE* promoter, whereas red rectangles are *CDF5* exons and dark green rectangles are *FLORE* exons. (+) and (-) represent sense and antisense strands, respectively. Expression of *CDF5* under the control of the *FLORE* promoter in a *cdf5-5'utr* mutant results in *CDF5* transcript accumulation throughout the day **(b)** and the inhibition of the *FLORE* waveform **(c)**, as determined by qPCR (quantitative real time reverse-transcription PCR) normalized with *Actin2*. Results shown are the means ± SD (Standard Deviation) of three technical repeats in one representative experiment out of two biological replicates. Grey rectangles represent the dark period and Time (h) represents hours after lights on.

159x279mm (300 x 300 DPI)

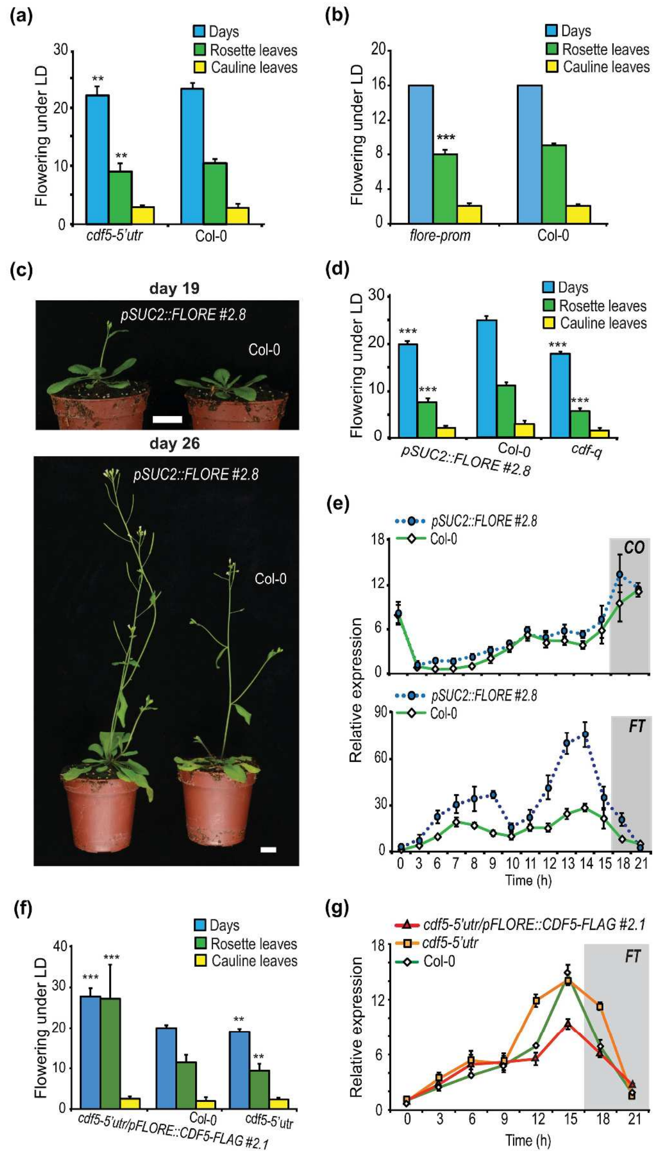

Figure 5. Modulation of *Arabidopsis CDF5 (CYCLING DOF FACTOR 5)* and *FLORE (CDF5 LONG NON-CODING RNA)* transcript levels affects flowering under long days. (a) Depletion of *CDF5* transcript in the *cdf5-5'utr* mutant results in a slightly early flowering phenotype (Student's t-test, $^{**}P<0.05$), measured in number of days (blue), rosette (green) and cauline leaves (yellow), in two biological replicates analysed (n=21). Each biological replicate included ten WT (Wild-Type, Col-0) plants, unless otherwise stated. **(b)** Modulation of *FLORE* transcript levels in *flore-prom* mutant plants grown under long day conditions alters flowering time determined by rosette leaf number (Student's *t*-test, $^{***}P<0.001$). Flowering time was evaluated by three parameters exactly as described above, in three independent experiments (n=47) with thirty-three WT plants as control. **(c, d)** *pSUC2*-driven overexpression of *FLORE* induces early flowering under long day conditions measured in number of days (blue), rosette leaf (green) and cauline leaf (yellow) number (Student's *t*-test $^{***}P<0.0001$). The flowering phenotype was visible as early as 19 days after transfer to long day conditions **(c)** and confirmed in two biological duplicates (n=24) **(d)**. The *cdf-q* mutant was used as a control for the early flowering phenotype. Scale bar 1 cm. qPCR

(quantitative real time reverse-transcription PCR) analysis showed that this phenotype correlated with a higher increase in *FT (FLOWERING LOCUS T)* expression levels but with a smaller change in *CO (CONSTANS)* transcript accumulation **(e)**. qPCR results were normalized with respect to *Actin2* and presented as the mean ± SD (Standard Deviation) of three technical replicates in one representative experiment out of two biological duplicates analysed. **(f)** Expressing *CDF5* under the control of the *FLORE* promoter in a *cdf5-5'utr* mutant resulted in delayed flowering under long days evaluated as number of days (blue), rosette leaf (green) and cauline leaf (yellow) numbers (n=20) in a representative experiment out of two biological replicates where two independent lines were analysed (Student's *t*-test **$P<0.05$; *** $P<0.005$). **(g)** The delayed flowering phenotype was associated with a decrease in *FT* transcript levels as determined by qPCR. These results were analysed as described above. Grey rectangles represent the dark period and Time (h) indicates the hours after lights on.

260x450mm (300 x 300 DPI)

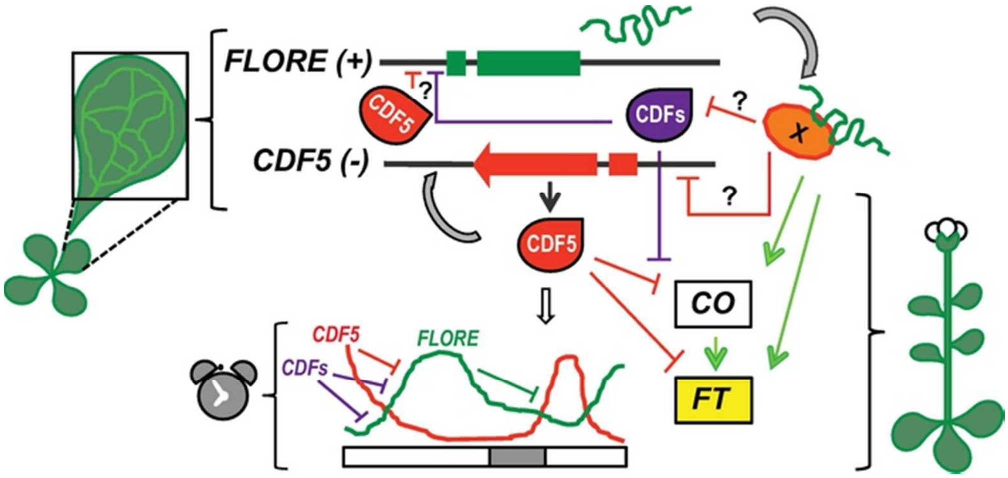

Figure 6. Model of *CDF5 (CYCLING DOF FACTOR 5)* and *FLORE (CDF5 LONG NON-CODING RNA)* mutual regulation in *Arabidopsis*. *CDF5* and *FLORE* constitute a circadian-regulated NAT (Natural Antisense Transcript) pair with an antiphasic pattern of expression. This is a consequence of mutual inhibition; *CDF5* inhibits *FLORE* accumulation in the afternoon, whereas *FLORE* represses *CDF5* in the morning. In addition, other *CDF*s [*CDF1 (CYCLING DOF FACTOR 1)*, *CDF2 (CYCLING DOF FACTOR 2)*, *CDF3 (CYCLING DOF FACTOR 3)*] could repress *FLORE* both in the morning and afternoon (purple lines). On the other hand, *FLORE* could also act as their negative regulator. Both *CDF5* and *FLORE* transcripts accumulate in the vascular tissue where they oppositely regulate the *CO (CONSTANS) - FT (FLOWERING LOCUS T)* module and consequently flowering time. Straight-end lines depict repression, whereas green arrows indicate induction. The oscillation patterns of *CDF5* (red) and *FLORE* (green) are also depicted. Open questions in the model are marked with (?). Grey rectangle represents the dark period under LDs (Long Days).

59x27mm (300 x 300 DPI)